2012-10

Infrared imaging using arrays of SiO2 micromechanical detectors

Datskos, P.G.; Lavrik, N.V.; Hunter, S.R.; Rajic, S.; Grbovic, D.

http://hdl.handle.net/10945/44115

Infrared imaging using arrays of SiO_2 micromechanical detectors

P. G. Datskos,[1,2,*] N. V. Lavrik,[1,2] S. R. Hunter,[1] S. Rajic,[1] and D. Grbovic[3]

[1]Oak Ridge National Laboratory, Oak Ridge, Tennessee 37931-6054, USA

[2]University of Tennessee, Knoxville, Tennessee 37996-1200, USA

[3]Department of Physics, Naval Postgraduate School, 833 Dyer Road, Monterey, California 93943, USA

*Corresponding author: datskospg@ornl.gov

Received June 21, 2012; revised August 13, 2012; accepted August 13, 2012;
posted August 14, 2012 (Doc. ID 171066); published September 19, 2012

In this Letter, we describe the fabrication of an array of bimaterial detectors for infrared (IR) imaging that utilize SiO_2 as a structural material. All the substrate material underneath the active area of each detector element was removed. Each detector element incorporates an optical resonant cavity layer in the IR-absorbing region of the sensing element. The simplified microfabrication process requires only four photolithographic steps with no wet etching or sacrificial layers. The thermomechanical deflection sensitivity was 7.9×10^{-3} rad/K, which corresponds to a noise equivalent temperature difference (NETD) of 2.9 mK. In the present work, the array was used to capture IR images while operating at room temperature and atmospheric pressure without the need for vacuum packaging. The average measured NETD of our IR detector system was approximately 200 mK, but some sensing elements exhibited an NETD of 50 mK.

OCIS codes: 040.1240, 310.1860.

Micromechanical IR detectors based on thermally sensitive bimorphs have proliferated significantly in the last several years. Focal plane arrays (FPAs) of such devices with optical [1–7] and capacitive [8] readouts were used as uncooled IR imagers in a series of recent efforts. Fabrication of micromechanical IR detectors is scalable to multimegapixel arrays [9]. Therefore, micromechanical FPAs hold the promise of high-resolution imaging devices at significantly reduced cost.

Silicon nitride (SiN_x) is frequently used as a structural material for micromechanical thermal detectors. Well-developed deposition processes and strong absorption in the wavelength region of 8 to 11 μm are key advantages for IR detection [7]. Thermal isolation is key in the operation of uncooled IR detectors. SiN_x has a thermal conductivity value between those of single-crystal Si and SiO_2. Typically, suspended SiN_x beams with less than 1 μm × 1 μm cross section and 20 to 50 μm length provide the thermal isolation sufficient for high-performance thermal imaging [2,7]. Optimizing the thermal isolation in uncooled IR detectors involves a challenging trade-off between low thermal conductivity and high stiffness. The benefit of using SiO_2 instead of SiN_x is the lower thermal conductivity. In fact, SiO_2 is characterized by the lowest thermal conductivity among all nonporous inorganic materials compatible with micromachining.

Other factors play a key role in the optimization of micromechanical IR imagers, such as the difference in thermal expansion for the bimaterial structure [10]. Another factor is the thermal isolation of each detector element. In this work, we used Al and SiO_2 as structural layers instead of the Au-coated SiN_x that was used previously. Al has a higher thermal expansion coefficient (23×10^{-6} K^{-1}) [11] compared to that for Au (14.2×10^{-6} K^{-1}) [2], and SiO_2 has a lower thermal conductivity value [12] (~1.4 Wm^{-1} K^{-1}) compared to that of SiN_x (19 Wm^{-1} K^{-1}) [2]. Furthermore, SiO_2 has a Young's modulus of 73.1 GPa, which is lower than that of SiN_x (~280 GPa). The Young's modulus for Al is 70 GPa compared to that for Au of 79 GPa. These lead to better thermal isolation and bimaterial responses for Al/SiO_2 structures when the thickness of the metal coating is a small fraction of the total cantilever thickness.

The FPAs discussed in this Letter used substrate-free structures with multifold IR micromechanical pixels that include an optical absorption cavity for IR imaging and have additional advantages [9]. Figure 1 illustrates the microfabricated detector. In the absorber area, an amorphous Si layer was embedded between the SiO_2 and Al layers. Using finite element analysis (FEA), we determined the resonant frequency and effective spring constant of the detector to be 2.78 kHz and 0.008 N/m, respectively. Thermal conductance was calculated to be 4.65×10^{-8} W/K, and the finite-element model calculation only considered conductive heat loss through the

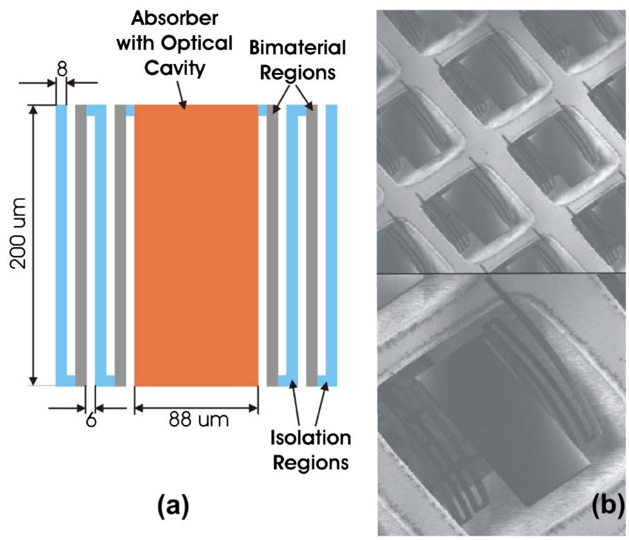

Fig. 1. (Color online) (a) Multifold structure was chosen in order to increase the effective lengths of both thermal isolation and bimaterial regions without increasing the overall detector size. (b) Micrograph images showing a single detector and part of the array.

0146-9592/12/193966-03$15.00/0

legs. This gave a thermomechanical responsivity of 4.1×10^{-3} rad/K and a thermal response time of 730 ms. It is worth noting that the predicted responsivity indicates a 70% improvement over devices of similar shape and size made of SiN_x and Au [3]. Using the relationships described previously [10], we estimated the noise-equivalent temperature difference (NETD) for the detector to be 1.2 mK excluding any influence of the CCD shot noise or heat loss mechanisms other than conduction. The scene temperature was 300 K with $F/1$ optics. Each element was 88 μm × 200 μm while the spectral absorption was dominated by the optical cavity. These estimates assumed that the only heat-loss mechanism was conduction through the supporting elements. Our measured values include the effect of all heat-conduction mechanisms.

A four-step photolithography process was used to microfabricate the FPAs. Compared to previous work [9], an additional photolithography step was introduced in order to create the optical cavity within the detector-absorbing region. The thickness of the optical cavity was optimized using a generalized Rouard method [13]. The optical cavity is formed by the layer of amorphous Si embedded between the SiO_2 and Al layers, and its thickness determines the IR-wavelength region, which in this work was centered at 10 μm [14]. Increasing the optical cavity finesse enhances the absorption of IR radiation in this spectral region. Micrographs of released structures are shown in Fig. 1(b); the images were taken using an FEI focused ion beam tool equipped with a liquid Ga source. The IR absorbers in these structures show improved flatness, which is very important because the optical readout of micromechanical detectors relies on the flatness of pixels in the FPA. The decreased deformation of the absorber region is due to the reduced total differential stress in the Al/α-Si/SiO_2 stack and possibly due to increased rigidity provided by the additional 1.1 μm layer of amorphous Si.

The experimental setup was similar to that used previously [9]. Laser light was focused on individual detectors, and the detector motion was observed using a photodetector (similar to those used in atomic force microscopy). The measured resonant frequency (first fundamental mode) was 2.1 kHz and is comparable to the value determined by FEA modeling. The experimentally measured thermal response time was 187 ms. This value corresponds to the thermal conductance between the detector and the environment of 1.8×10^{-7} W/K. Using the optical readout, the measured thermomechanical responsivity was 7.9×10^{-3} rad/K, which is almost double the value obtained using FEA modeling. The measured response time was 180 ms, which included both the convective and radiated heat loss. This discrepancy is attributed to deviations of the structural parameters and material properties from the nominal values used in the FEA modeling. In air, the quality factor Q was about 30 for the majority of detector elements studied. At 300 K and with $F/1$ optics, individual detectors in the array have an experimentally measured deflection sensitivity of 7.9×10^{-3} rad/K, while the fundamental limit for NETD was 2.97 mK.

The optical readout used in the present study was described previously [2]. A 1 megapixel CCD-array camera with a 10 bit dynamic range was used with a pixel size of 7.4 μm^2 and a sensitivity of 13 μV/electron. A series of images was captured while the pressure in the cell housing the FPA was varied from 15 mTorr to ambient. An IR image of a human hand at atmospheric pressure is shown in Fig. 2. The separation between active areas in the image is due to the particular design of the Si frame surrounding each pixel providing the structural support. The quality of the image and uniformity of the FPA response can be substantially improved by minimizing the differential stress between Al and SiO_2 and refining the microfabrication sequence.

The calculated NETD values indicate that high-performance micromechanical IR imagers under ambient conditions are possible. In order to verify this experimentally, we performed an aggregate measurement of the performance of multiple detectors in the array by observing the brightness of the CCD pixels while varying the temperature (10 K above ambient) of a target placed in front of the imaging system. The measured values of NETD for each pixel were obtained using $\text{NETD} = I_n/I_s(T_T - T_B)$. I_n is the level of noise measured for each pixel in the CCD, I_s is the signal intensity for a certain target temperature, while T_T and T_B are the temperatures of the target and the background, respectively. The resulting histograms showed that the peak values of NETD for the system, including the readout, were approximately 200 mK at 10 mTorr pressure (Fig. 3). However, some pixels showed NETD values below 50 mK. The difference between the measured and calculated NETD are attributed to CCD noise.

In summary, we have demonstrated the feasibility of SiO_2-based micromechanical IR detectors capable of theoretically approaching performance levels of commercial uncooled detectors. Some pixels of the fabricated FPA exhibited NETD values as low as 50 mK. An important advantage of the present approach is the straightforward microfabrication sequence that does not involve wet etching, and is material-selection tolerant, allowing further performance optimization. It is important to point out that the unprocessed raw images reported in this Letter were obtained without employing any image processing to enhance the perceived image quality. In

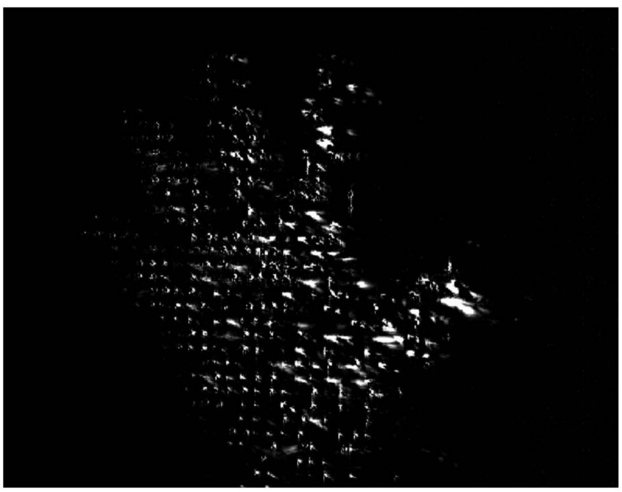

Fig. 2. Thermal image of a human hand obtained using an optical readout at atmospheric pressure and temperature.

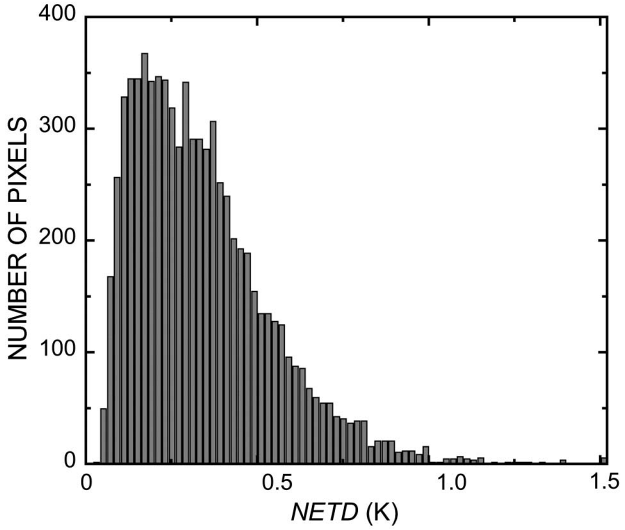

Fig. 3. NETD histograms show that the peak number of individual detector elements exhibit NETD values of less than 200 mK, with some devices showing less than 50 mK.

this particular case the poor fill factor of our design also contributes to the image quality.

The work performed was supported by the Laboratory Director's Research and Development Program of Oak Ridge National Laboratory. Microfabrication was performed in part at Cornell NanoScale Facility. A portion of this research was conducted at the Center for Nanophase Materials Sciences, which is sponsored at Oak Ridge National Laboratory by the Scientific User Facilities Division, Office of Basic Energy Sciences, U.S. Department of Energy. Oak Ridge National Laboratory is operated for the U.S. Department of Energy by UT-Battelle under Contract No. DE-AC05-00OR22725.

References

1. F. Dong, Q. Zhang, D. Chen, L. Pan, Z. Guo, W. Wang, Z. Duan, and X. Wu, Sens. Actuat. A **133**, 236 (2007).
2. D. Grbovic, N. V. Lavrik, P. G. Datskos, D. Forrai, E. Nelson, J. Devitt, and B. McIntyre, Appl. Phys. Lett. **89**, 073118 (2006).
3. Z. Guo, F. D. Q. Zhang, D. Chen, Z. Xiong, Z. Miao, C. Li, B. Jiao, and X. Wu, Sens. Actuat. A **137**, 13 (2007).
4. T. Ishizuya, J. Suzuki, K. Akagawa, and T. Kazama, in *The Fifteenth IEEE International Conference on Micro Electro Mechanical Systems* (IEEE, 2002), p. 578.
5. J. Salerno, Proc. SPIE **6542**, 65421D (2007).
6. S. Shi, B. Jiao, D. Chen, C. Li, D. Ding, Y. Ou, T. Ye, Z. Duan, X. Wu, and Q. Zhang, Sens. Actuat. A **133**, 64 (2007).
7. Y. Zhao, R. H. M. Mao, A. Majumdar, J. Varesi, P. Norton, and J. Kitching, J. Microelectromech. Syst. **11**, 136 (2002).
8. S. R. Hunter, G. Maurer, L. Jiang, and G. Simelgor, Proc. SPIE **6206**, 62061J (2006).
9. D. Grbovic, N. V. Lavrik, S. Rajic, and P. G. Datskos, J. Appl. Phys. **104**, 054508 (2008).
10. P. G. Datskos, N. V. Lavrik, and S. Rajic, Rev. Sci. Instrum. **75**, 1134 (2004).
11. F. Kroeger and C. Swenson, J. Appl. Phys. **48**, 853 (1977).
12. K. Goodson, M. Flik, L. Su, and D. A. Antoniadis, IEEE Electron Device Lett. **14**, 490 (1993).
13. P. Lecaruyer, E. Maillart, M. Canva, and J. Rolland, Appl. Opt. **45**, 8419 (2006).
14. D. Grbovic, "Imaging by detection of infrared photons using arrays of uncooled micromechanical detectors," Ph.D. dissertation (University of Tennessee, 2008).